Sparse Generalized Pencil of Function and its application to system identification and structural health monitoring

Reza Mohammadi-Ghazi[a] and Oral Büyüköztürk[b]

[a]Doctoral candidate, Massachusetts Institute of Technology, Building 1-170, 77 Massachusetts Avenue, Cambridge, MA, USA
[b]Professor, Massachusetts Institute of Technology, Building 1-281, 77 Massachusetts Avenue, Cambridge, MA, USA

ABSTRACT

Singularity expansion method (SEM) is a system identification approach with applications in solving inverse scattering problems, electromagnetic interaction problems, remote sensing, and radars. In this approach, the response of a system is represented in terms of its complex poles; therefore, this method not only extracts the fundamental frequencies of the system from the signal, but also provides sufficient information about system's damping if its transient response is analyzed. There are various techniques in SEM among which the generalized pencil-of-function (GPOF) is the computationally most stable and the least sensitive one to noise. However, SEM methods, including GPOF, suffer from imposition of spurious poles on the expansion of signals due to the lack of apriori information about the number of true poles. In this study we address this problem by proposing sparse generalized pencil-of-function (SGPOF). The proposed method excludes the spurious poles through sparsity-based regularization with ℓ_1-norm. This study is backed by numerical examples as well as an application example which employs the proposed technique for structural health monitoring (SHM) and compares the results with other signal processing methods.

Keywords: Singularity expansion method, generalized pencil of function, complex poles, regularization, sparsity, lasso regression, energy leakage

1. INTRODUCTION

In signal processing domain, the Fourier transform (FT) is the most dominant technique for its simplicity and high efficiency. Linearity and stationarity are the two main assumptions in FT which result in imposition of spurious harmonics on the expansion of signals and hence, leakage of energy. Several techniques such as the wavelet transform (WT) and the Hilber-Huang transform (HHT) have been proposed to overcome this issue for analyzing non-stationary and/or nonlinear signals. WT is an efficient technique for characterizing non-stationary signals, but the energy leakage is inevitable in this method due to the assumption of linearity. The HHT goes one step further by providing the highest possible time-frequency resolution for frequency spectrum without any assumption of linearity or stationarity.[1] However, this method is computationally intensive due to the iterative use of spline interpolations. Moreover, the results of HHT for a signal may considerably vary by changing the algorithm's tuning parameters as the HHT does not have a closed form mathematical formula. Besides the pros and cons of these methods, none of them provide information about damping of the system being studied.

An alternative approach to the above mentioned ones is singularity expansion method (SEM) which characterizes a system's response in terms of the singularities in the complex-frequency plane.[2,3] Such characterization provides sufficient information about system damping when its transient response is analyzed. The main subcategories of SEM for extracting systems' complex poles and their associated residues are Prony method,[4] Jain's pencil-of-function (POF) method[5,6] and its improved version,[7] ESPRIT,[8] and generalized pencil-of-function (GPOF).[9] Although method have made major impacts mainly on solving inverse scattering problems, they

suffer from two issues: 1) they are generally sensitive to noise, and 2) the number of system's complex poles should be known apriori. The first issue has been solved to an extend in the GPOF. Moreover, this method is computationally more stable and less demanding compared to that others listed above; however, it still requires the system order to be known a priori. Underestimation and overestimation of the system order, respectively, result in high errors in estimating the poles and imposition of spurious damped harmonics to the expansion of signal and hence, energy leakage. The proposed solutions for estimating the number of poles[9–14] usually require information about the noise characteristics and none of them guarantees the best prediction for the number of true poles as they hard threshold them. This motivates further investigations on developing robust system order determination techniques to be used along with SEM methods.

In SEM, the complex poles, which represent the damped harmonic modes of the system, are extracted from the signal and hence, the extracted modes are not orthogonal to the signal. Therefore, the least square (LS) method, which is commonly used for computing the corresponding residues, never push any of them to hard zero. In this study, we consider sparsity-based regularization with ℓ_1 norm as the basis for computing the residues. By incorporating this technique into GPOF we propose sparse generalized pencil-of-function (SGPOF). With the ℓ_1-norm regularization, the residues associated with the insignificant poles are pushed to zero and hence, the energy leakage will be minimized due to the sparse property of SGPOF. This brings various additional applications for this method such as system order determination and feature extraction for structural health monitoring (SHM). The body of the paper starts with a review of GPOF and the description of the problem that is addressed in this study. The SGPOF algorithm and its technicalities will be discussed in section 3 followed by section 4 which proposes an algorithm for determining optimal parameters of SGPOF. Finally, various numerical and application examples are presented in section 5 and the results are compared with other signal processing methods.

2. REVIEW OF GPOF AND PROBLEM DESCRIPTION

2.1 Review of GPOF

Considering T_s as the sampling period and $k = 0, 1, \cdots, N-1$, a discrete signal $y(kT_s)$ can be expanded in term of damped sinosoids , i.e.,

$$y(kT_s) \approx \sum_{m=1}^{M} R_m e^{s_m k T_s} = \sum_{m=1}^{M} R_m z_m^k \tag{1}$$

where M is the number of poles, R_m are the residues, and $s_m = \alpha_m + j\Omega_m$ are the complex poles. The pencil-of-function method considers $L+1$ number of linearly independent vectors $\{\mathbf{y_0}, \mathbf{y_1}, \cdots, \mathbf{y_L}\}$ where $\mathbf{y_m} = [y(m), y(m+1), \cdots, y(m+N-L-1)]^T$ and the superscript T denotes matrix transpose. By arranging these vectors, known as "information" vectors,[6] the following matrices are defined[9]

$$\mathbf{Y_1} = [\mathbf{y_0}, \mathbf{y_1}, \cdots, \mathbf{y_{L-1}}] \tag{2}$$
$$\mathbf{Y_2} = [\mathbf{y_1}, \mathbf{y_2}, \cdots, \mathbf{y_L}] \tag{3}$$

It has been proven that the poles are the generalized eigenvalues of of the matrix pencil[9] , $\mathbf{Y_2} - z\mathbf{Y_1}$, which implies that the parameters z_m can be obtained by solving the followig generalized eigenvalue problem

$$\mathbf{Y_1}^+\mathbf{Y_2} - z\mathbf{I} \tag{4}$$

where the superscript $+$ denotes the Moore-Penrose pseudo-inverse. The proposed approach in standard GPOF for excluding the spurious poles is to keep only the first M largest eigenvalues of (4) and form the vector $\mathbf{z}_0$ as

$$\mathbf{z}_0 = [z_1, z_2, \cdots, z_M] \tag{5}$$

The corresponding residues for the poles in $\mathbf{z}_0$ are determined through LS as[9]

$$\begin{bmatrix} y(1) \\ y(2) \\ \vdots \\ y(N-1) \end{bmatrix} = \begin{bmatrix} 1 & 1 & \cdots & 1 \\ z_1 & z_2 & \cdots & z_M \\ z_1^2 & z_2^2 & \cdots & z_M^2 \\ \vdots & \vdots & & \vdots \\ z_1^{N-1} & z_2^{N-1} & \cdots & z_M^{N-1} \end{bmatrix} \begin{bmatrix} R_1 \\ R_2 \\ \vdots \\ R_M \end{bmatrix} \tag{6}$$

which can be rewritten as

$$\mathbf{y} = \mathbf{Z} \cdot \mathbf{R} \tag{7}$$

2.2 Problem description

In addition to the number of poles, the GPOF method makes use of another free parameter L which controls the shape of information matrices. The advantage of GPOF over POF method[6] is a result of this parameter and in the case of $L = M$ the two methods become the same. The accuracy of GPOF depends highly on the right choice of L and based on some numerical analysis, it was shown[9] that GPOF works best when L is around $N/2$. This result is based on a first order perturbation analysis that assumes the corresponding residues for all entries of $\mathbf{z}_0$ is non-zero. This assumption can be violated when sparsity-based regularization is used instead of LS and hence, the optimal L may no longer be around $N/2$. To solve this problem, we will first establish a technique to distinguish the true poles from the spurious ones. Secondly, a method is proposed for finding the optimal shape parameter, L, using the Akaike information criterion (AIC).

3. SPARSE GENERALIZED PENCIL-OF-FUNCTION

For the moment, assume that the parameter L is given. Instead of hard-thresholding, the spurous poles can be excluded via regularized least square (RLS) with ℓ_1-norm. For that, the LS in (6) and (7) can be replaced by the following optimization problem

$$\underset{\mathbf{R} \subset \mathbb{C}^M}{\arg\min} \|\mathbf{Z} \cdot \mathbf{R} - \mathbf{y}\|_2^2 + \lambda_c \|\mathbf{R}\|_1 \tag{8}$$

where $\mathbb{C}$ is the domain of complex numbers. $\|\cdot\|_1$ is the ℓ_1-norm operator and λ_c is the regularization parameter for optimization in complex domain. There is no need to threshold the eigen values of the matrix pencil and all singular values obtained from (4) are included in (8). Both $\mathbf{Z}$ and $\mathbf{R}$ in (8) are complex valued matrices; thus, the solution of this optimization problem is not as straightforward as in real-valued lasso. Several methods have been proposed for complex lasso[15–17]; however, they generally suffer from the computational intensity and/or lack of considering the physics of the problem. One such physical phenomena is that the poles of a physical system appear in complex conjugate pairs[11, 12, 14]. Using this fact, one can change the complex-valued optimization of (8) into a real-valued lasso. To do that, assume there are $\widetilde{m}$ number of poles that appear as complex conjugate pairs in $\mathbf{z}_0$. By excluding the poles without complex conjugate from $\mathbf{z}_0$, the vector $\widetilde{\mathbf{z}}_0$ is defined as

$$\widetilde{\mathbf{z}}_0 = \left\{ \widetilde{z}_l = z_m \in \mathbf{z}_0 | z_m^H \in \mathbf{z}_0 \; ; \; m = 1, \cdots, M \right\} \tag{9}$$

where $l = 1, \cdots, \widetilde{m}$. Note that the entries of $\widetilde{\mathbf{z}}_0$ are sorted based on their magnitude and hence, the indices of the complex conjugate pairs are different by one, i.e., $\widetilde{z}_{2i} = \widetilde{z}_{2i-1}^H$ with $i = 1, \cdots, \widetilde{m}/2$. By considering $\widetilde{\mathbf{z}}_0$ instead of $\mathbf{z}_0$, (8) is converted to

$$\underset{\widetilde{\mathbf{R}} \subset \mathbb{C}^{\widetilde{m}}}{\arg\min} \left\| \widetilde{\mathbf{Z}} \cdot \widetilde{\mathbf{R}} - \mathbf{y} \right\|_2^2 + \widetilde{\lambda}_c \left\| \widetilde{\mathbf{R}} \right\|_1 \tag{10}$$

where

$$\widetilde{\mathbf{Z}} = \begin{bmatrix} 1 & 1 & \cdots & 1 \\ \widetilde{z}_1 & \widetilde{z}_2 & \cdots & \widetilde{z}_{\widetilde{m}} \\ \widetilde{z}_1^2 & \widetilde{z}_1^2 & \cdots & \widetilde{z}_{\widetilde{m}}^2 \\ \vdots & \vdots & & \vdots \\ \widetilde{z}_1^{N-1} & \widetilde{z}_2^{N-1} & \cdots & \widetilde{z}_{\widetilde{m}}^{N-1} \end{bmatrix} \text{ and } \widetilde{\mathbf{R}} = \begin{bmatrix} \widetilde{R}_1 \\ \vdots \\ \widetilde{R}_{\widetilde{m}} \end{bmatrix} \tag{11}$$

where $\widetilde{\lambda}_c$ is the regularization parameter for the new complex-valued optimization of (10). Recaling the main idea of SEM, represented in (1), $\mathbf{y}$ can be expanded in terms of exponentially damped harmonics of the form

$$A_i e^{\zeta_i t} \sin(\omega_i t + \theta_i) \tag{12}$$

ω_i and ζ_i are respectively the frequency and damping associated with $\widetilde{z}_{2i-1}$ and its complex conjugate, $\widetilde{z}_{2i}$; i.e. for discrete signals $\omega_i = |\ln(\widetilde{z}_{2i-1}/T_s)| = |\ln(\widetilde{z}_{2i}/T_s)|$ and $\zeta_i = -\cos(\angle \ln(\widetilde{z}_{2i-1})) = -\cos(\angle \ln(\widetilde{z}_{2i}))$. A_i and θ_i, the amplitude and phase of the damped harmonic modes, depend on the complex residue $\widetilde{R}_i$ which

should be estimated by solving the RLS problem of (10). The harmonic function of the form (12) is a linear combination of $\sin(\omega_i t)$ and $\cos(\omega_i t)$ based on the simple trigonometric equation that $A_i e^{\zeta_i t} \sin(\omega_i t + \theta_i) = A_i e^{\zeta_i t} \left[\cos(\theta_i)\sin(\omega_i t) + \sin(\theta_i)\cos(\omega_i t)\right]$. Thus, $\widetilde{\mathbf{Z}}$ in (10) can be equivalently replaced by a real-valued matrix $\mathbf{S}$ which is

$$\mathbf{S} = S_{k,l} \tag{13}$$

where

$$S_{k,l} = \begin{cases} e^{\zeta_i k T_s}\sin(\omega_i k T_s) & \text{if } l = 2i - 1 \\ e^{\zeta_i k T_s}\cos(\omega_i k T_s) & \text{if } l = 2i \end{cases} \tag{14}$$

where $k = 1, \cdots, N - 1$. Using $\mathbf{S}$, the RLS in (10) can be converted into an equivalent real-valued optimization as

$$\underset{\mathbf{B} \subset \mathbb{R}^{\widetilde{m}}}{\arg\min} \|\mathbf{S} \cdot \mathbf{B} - \mathbf{y}\|_2^2 + \lambda_r \|\mathbf{B}\|_1 \tag{15}$$

where $\mathbf{B}$, the vector of unknown coefficients, is

$$\mathbf{B} = \begin{bmatrix} A_1 \cos(\theta_1) \\ A_1 \sin(\theta_1) \\ \vdots \\ A_{\widetilde{m}/2} \cos(\theta_{\widetilde{m}/2}) \\ A_{\widetilde{m}/2} \sin(\theta_{\widetilde{m}/2}) \end{bmatrix}_{\widetilde{m} \times 1} \tag{16}$$

and λ_r is the regularization parameter for the real-valued lasso. The corresponding residues of the poles in $\widetilde{\mathbf{z}}_0$ can be determined by applying the Euler's formulafrom to the entries of $\mathbf{B}$.

4. FINDING THE OPTIMAL SHAPE PARAMETER L

The problem of optimizing L is coupled with the minimization problem of (15) and hence, solving both problems simultaneously is not straightforward. Therefore, a simple grid search method is used for finding the optimal value of L. For each value in the grid, the corresponding poles and residues are determined as described in the previous section. Then, the best model is chosen by the Akaike Information Criterion (AIC) which is[18]

$$\text{AIC} = N \ln\left(\widehat{\sigma}_{mle}^2\right) + 2p \tag{17}$$

where $\widehat{\sigma}_{mle}^2$ is the maximum likelihood estimate of the residual error variance, $\mathbf{S} \cdot \mathbf{B} - \mathbf{y}$, and p is the number of true poles for each model. If the residual error is normally distributed, (17) can be modified for finite dimensional problem as[19]

$$\text{AIC}_f = \text{AIC} + \frac{2p(p+1)}{N - p - 1} \tag{18}$$

The model with the lowest information criterion has the optimal parameter L. In practice, the model with AIC about one standard deviation larger than the best model is selected.

5. APPLICATION EXAMPLES

Apart from determination of system fundamental frequencies and damping in the case of analyzing its transient response, the sparse property of SGPOF brings a wide range of applications for this method. System order determination and providing damping spectrum are two such applications of SGPOF. In this section, some application examples of SGPOF for system identification and SHM are presented and the results are compared with other methods.

5.1 Two sinusoidal waves with a spike

Similar to short-time FFT, one can define short-time SGPOF by windowing signals. This examples shows the efficacy of short-time SGPOF in detecting the discontinuities either in amplitude or frequency of signals. Let $y_1(t)$ to be

$$y_1(t) = \begin{cases} \sin(2\pi f_1 t) \; ; \; t \neq 0.1875 \\ 1.5 \; ; \; x = 0.1875 \end{cases} \; ; f_1 = \begin{cases} 500 \; ; \; t < 0.125 \\ 1000 \; ; \; t \geq 0.125 \end{cases} \tag{19}$$

where f_1 is frequency in Hz. The signal is shown in Fig.1. The results of analyzing $y_1(t)$ with sampling frequency of $T_s = 0.00005$ sec by HHT, FT, and short-time SGPOF are shown in Fig.2. f_1, ℓ, and τ in this figure denote frequency, size of window, and window overlap, respectively. The trade-off between the temporal and frequency resolutions of the FFT is obvious in this figure. Basically, the FFT can either detect the discontinuity in frequency or time, because improving the accuracy of one decreases the accuracy of the other (Fig.2(a) and 2(b)). Hilbert spectrum, which is shown in Fig.2(c), provides the highest possible resolution for time and frequency simultaneously. The sparsity in HHT is not guaranteed, but the method usually represents the signals in terms of limited number of nonlinear functions called intrinsic modes (IMFs) if the parameters for extracting these modes are tuned appropriately. Although the accuracy and interpretablity of HHT results depend highly on those tuning parameters, there is no single method for determining the appropriate values for them. Moreover, HHT is computationally intensive, does not provide any information about the systems' damping, and its results are sometimes difficult to interpret. Note that, the definition of frequency in HHT is different from Fourier domain, however the same units for this quantity are used in all figures. The SGPOF frequency spectrum, shown in Fig.2(d), implies that the proposed method provides a sparse spectrum without energy leakage. Furthermore, the method is capable of detecting both the frequency shift and the spike. However, as it is shown in this figure, SGPOF did not eliminate all spurious poles at the point of frequency shift. The reason for that is the inherent stationarity assumption of short-time SGPOF as a result of windowing.
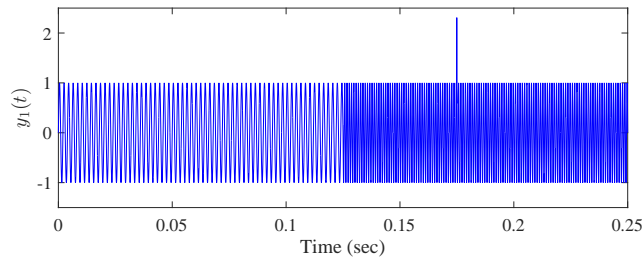

Figure 1. The two sinusoidal waves with a spike, $y_1(t)$

5.2 Application to SHM

The sparse property of SGPOF, which avoids energy leakage by excluding spurious modes, makes it appropriate for use in SHM with energy-based technique. For more information on the energy-methods in SHM and the importance of sparsity the readers are referred to[20] . In addition to sparsity, SGPOF directly provides information about the real-parts of the poles. In this part, we use this feature and compare it with auto-regressive (AR) coefficients[21,22] for damage detection in a plate structure. The experimental setup involved a shaker, high-speed camera, and extra lighting as shown in Fig.3(a). The details of the specimens are also shown in Fig.3(b) and 3(c). The plate is bolted to a concrete base and the shaker excited the plate with a white Gaussian noise waveform in a horizontal direction in the video. After the plate vibration reached steady state, 3.5 seconds of video was recorded at 2000 frames per second using the high speed camera. The screenshots of the intact and the notched elements are respectively shown in Fig.4(a) and 4(b). The displacement filed of both the intact and the notched plates were extracted using the procedure which is described in[23,24] . A set of 100 pixels in the form of a 20×5 planar grid on the screenshot of the plates were chosen as the pseudo-sensor location (Fig. 4(c)). The displacement time-series of these points were processed by SGPOF and the complex poles were extracted. The real and imaginary parts of the poles were used as the damage sensitive features to be fed as the input to the graphical model based algorithm described in[25] . As it is shown in Fig.4(d), the damage can be perfectly
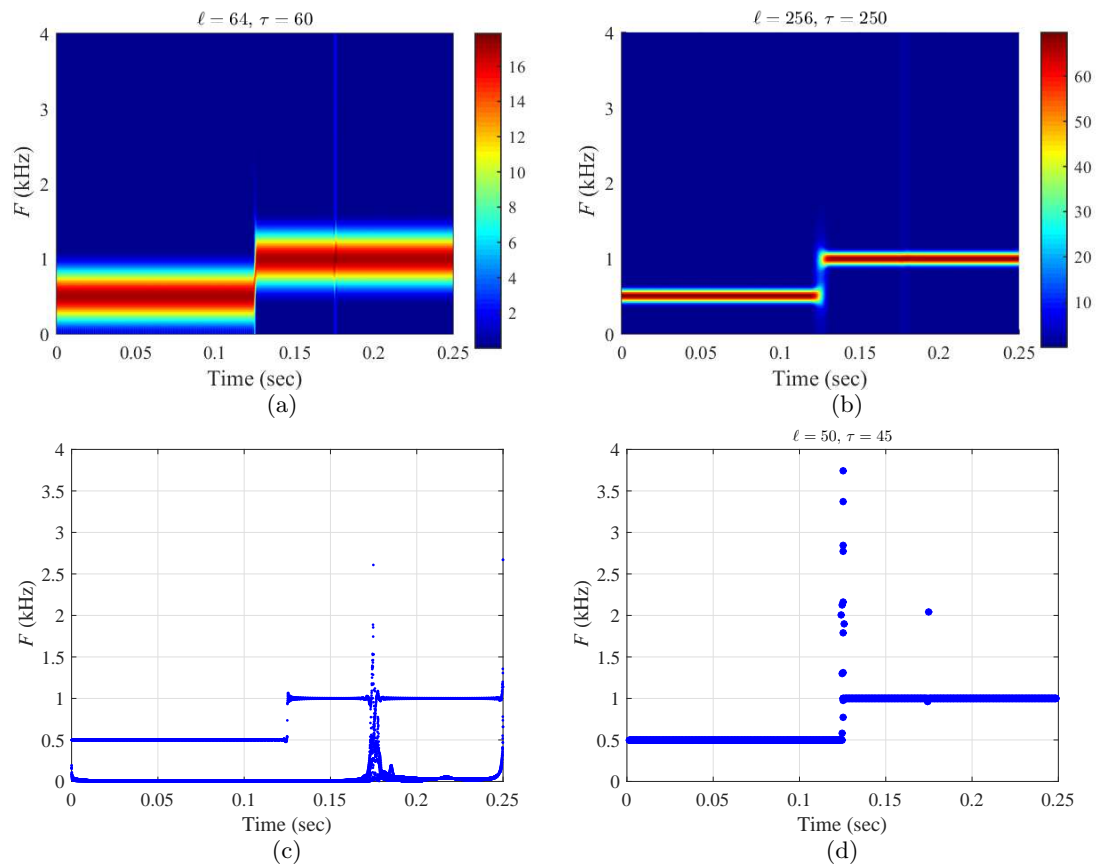
Figure 2. The results of analyzing $y_1(t)$; (a) Fourier spectrum with $\ell = 64$ and $\tau = 60$; (b) Fourier spectrum with $\ell = 256$ and $\tau = 250$; (c) Hilbert spectrum; (d) SGPOF spectrum with $\ell = 50$ and $\tau = 45$.
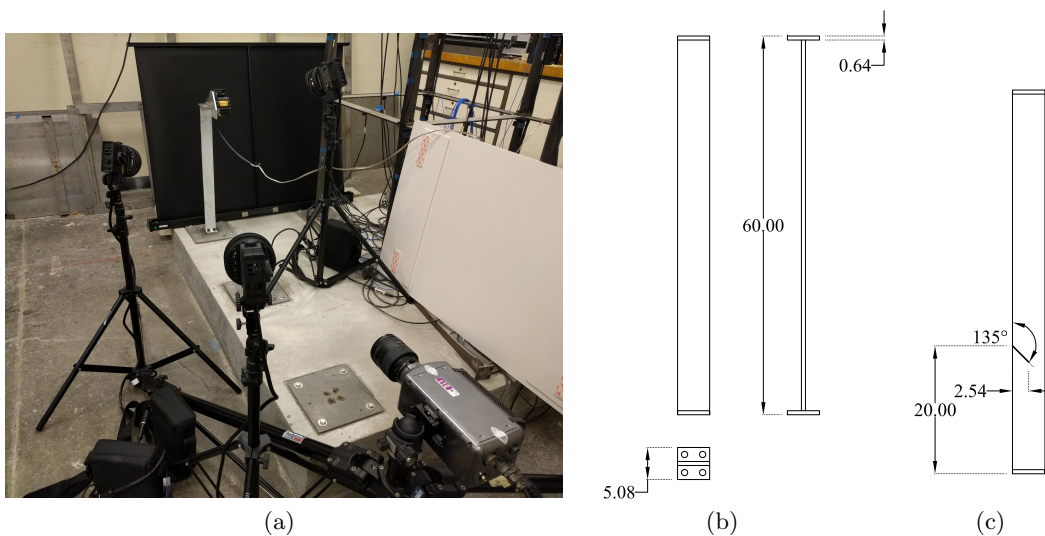

Figure 3. Picture of the experimental setup for the plate structure and the speciments, (a) shows the plate fixed to a concrete base, the shaker bolted to the top of the plate, high-speed camera, and extra lighting, (b) dimensions of the plate, (c) position and configuration of the notch on the plate

localized using the poles of the system as the damage sensitive feature. The system's complex poles at the tip of the notch before and after damage are shown in Fig.5(a) and 5(b). It follows from this figure that the real part of the poles are considerably more sensitive to the damage than the complex parts which is affected dominantly by frequency. This confirms the importance of the information about the real part of the poles provided by SEM methods for the sake of system identification.

In order to compare the efficacy of SGPOF with other methods in capturing the changes of structural properties, the same analysis were performed using AR coefficients. A tree-based feature selection method was used to conduct this comparison. For that, both the SGPOF and AR features were fed into a a gradient boosting model[26] with 300 estimators, learning ration of 0.1, and the maximum length of 6 for the decision trees. The feature importance results computed by the gradient boosting model is shown in Fig.5(c). It follows from the figure that the effects of damage are better manifested in SGPOF feature compared to AR model. Note that the relevancy of features is problem dependent and these results may not be generalizable for other structures.
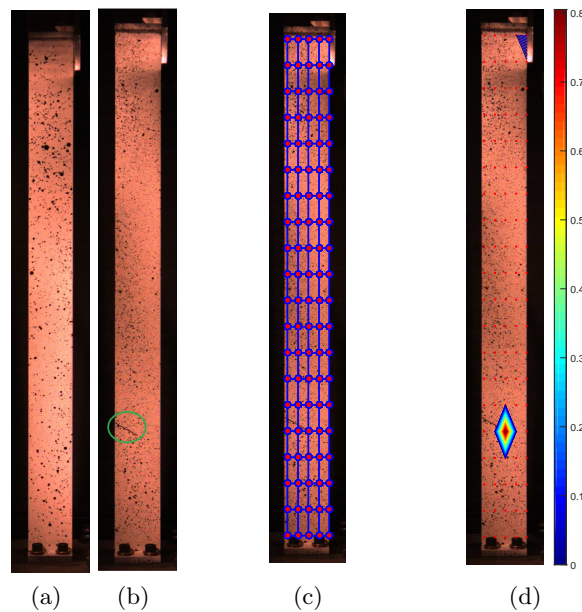

(a)   (b)   (c)   (d)

Figure 4. the specimens, the location of pseudo-sensors, and the graphical model used for damage detection; (a) screenshot of the intact plate, (b) screenshot of the notched element with a green circle around the notch, (c) the pseudo-sensors grid points and the configuration of graphical model that is used for damage detection, (d) damage localization result

6. CONCLUSION

SGPOF was presented as a sparse extension to GPOF method and a solution to the problem associated with imposition of spurious poles in SEM techniques. The proposed method excludes the spurious harmonics using sparsity based regularization with ℓ_1-norm. Also, we provided an information-based technique for finding the optimal value of the pencil matrix shape parameter.

The comparison between the SGPOF, FT and HHT shows that the proposed method does not suffer from the trade-off between the temporal and frequency resolutions as much as FT does. Furthermore, contrary to HHT, the SGPOF guarantees sparsity because of using the ℓ_1-norm. However, SGPOF cannot conquer FT for its computational efficiency nor the HHT for the high resolution it provides for frequency spectrum. The result of damage detection using SGPOF damage sensitive features also shows the capability of the method for capturing the changes in the system's properties, especially through the variations in the real part of the poles.
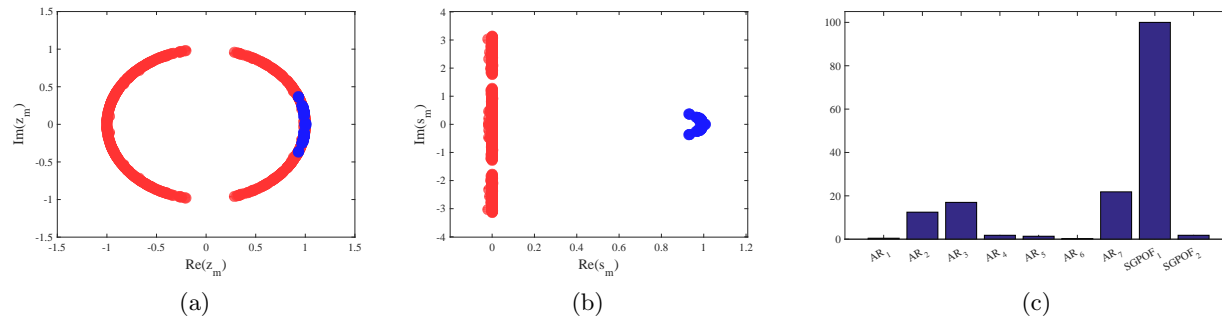
Figure 5. (a) real vs. imaginary part of parameter z before (blue) and after damage (red), (b) real vs. imaginary part of the poles, $\ln(z)$, before (blue) and after damage (red), (c) feature importance results of gradient boosting model for comparing SGPOF and AR damage sensitive features

Finding the optimal value for the pencil matrix shape parameter was conducted through a grid search and model selection using AIC. Having a mathematical formula for SGPOF brings the potential for further investigations for more efficient optimization techniques in order to determine the shape parameter.

ACKNOWLEDGMENTS

REFERENCES

[1] Huang, N., Shen, Z., Long, S. R., Wu, M. C., Shih, H. H., Zheng, Q., Yen, N., Tung, C. C., and Liu, H. H., "The empirical mode decomposition and the hilbert spectrum for nonlinear and non-stationary time series analysis," *Proceedings of the Royal Society Series A* (454), 903–995 (1998).

[2] Baum, C. E., [*On the singularity expansion method for solution to electromagnetic interaction problem*], Interaction Note 88 (Dec. 11 1971).

[3] Baum, C. E. and Felsen, L. B., [*Transient Electromagnetic Fiellds*], Springer-Verlag (1976).

[4] Van Blaricum, M. L. and Mitra, R., "A technique for extracting the poles and residues of a system directly from its transient response," *IEEE Transactions on Antennas and Propagation* **AP-23**(6), 777–781 (1975).

[5] Jain, V. K., Sarkar, T. K., and Weiner, D. D., "Rational modeling by pencil-of-functions method," *IEEE Transactions on Antennas and Propagation* **AP-28**(6), 928–933 (1980).

[6] Sarkar, T. K., Nebat, J., Weiner, D. D., and Jain, V. K., "Suboptimal approximation/identification of transient waveforms from electromagnetic systems by pencil-of-function method," *IEEE Transactions on Acoustics, Speech, and Signal Processing* **ASSP-31**(3), 564–573 (1983).

[7] j. Mackay, A. and McCoven, A., "An improved pencil-of-function method and comparisons with traditional methods of pole extraction," *IEEE Transactions on Antennas and Propagation* **AP-35**(4), 435–441 (1987).

[8] Roy, R. and Kailath, T., "Esprit-estimation of signal parameters via rotational invariance technique," *IEEE Transactions on Acoustics, Speech, and Signal Processing* **37**(7), 984–995 (1989).

[9] Hua, Y. and Sarkar, T. K., "Generalized pencil-of-function method for extracting poles of an em systemfrom its transient response," *IEEE Transactions on Antennas and Propagation* **37**(2), 229–234 (1989).

[10] Van Blaricum, M. L. and Mitra, R., "Problems and solutions associated with prony's method for processing transient data," *IEEE Transactions on Antennas and Propagation* **AP-26**(1), 174–182 (1978).

[11] Angkaew, T., Matsuhara, M., and Kumagai, N., "Finite-element analysis of waveguide modes: A novel approach that eliminates spurious modes," *IEEE Transactions on Microwave Theory and Techniques* **MTT-35**(2), 117–123 (1987).

[12] Yang, S., Deng, W., Yang, Q., Wu, G., and Suo, Y., "A frequency selection method based on the pole characteristics," *International Journal of Antennas and Propagation* , 1–8 (2013).

[13] Carriere, R. and Moses, R. L., "High resolution radar target modeling using a modified prony estimator," *IEEE Transactions on Antennas and Propagation* **40**(1), 13–18 (1992).

[14] Lee, J. and Kim, H., "Natural frequency extraction using generalized pencil-of-function method and transient response reconstruction," *Progress In Electromagnetics Research C* **4**, 65–84 (2008).

[15] Van Den Berg, E. and Freidlander, M. P., "Probing the pareto frontier for basis pursuit solutions," *Journal of Scientific Computing* **31**(2), 890–912 (2008).

[16] de Andrade, J. F., de Campos, M. L. R., and de Apolinario, J. A., "A complex version of the lasso algorithm and its application to beamforming," in [*The 7th International Telecommunications Symposium (ITS 2010)*], (2010).

[17] Maleki, A., Anitori, L., Yang, Z., and Baraniuk, R., "Asymptotic analysis of complex lasso via complex approximation message passing (camp)," *IEEE Transactions on Information Theory* **59**(7), 4290–4308 (2013).

[18] Chaurasia, A. and Harel, O., "Using aic in multiple linear regression framework with multiplyimputed data," *Health Serv Outcomes Res Methodol* **12**((2-3)), 219–233 (2012).

[19] Cavanaugh, J. E., "Unifying the derivations of the akaike and corrected akaike information criteria," *Statistics and Probability Letters* **31**, 201–208 (1997).

[20] Ghazi, R. M. and Buyukozturk, O., "Damage detection with small data set using energy-based nonlinear features," *Journal of Structural Control and Health Monitoring* (2015).

[21] Nair, K. K., Kiremidjian, A., and Law, K., "Time series-based damage detection and localization algorithm with application to the asce benchmark structure," *Journal of Sound and Vibration* **291**, 349–368 (2006).

[22] Nair, K. K. and Kiremidjian, A., "Time series based structural damage detection algorithm using gaussian mixtures modeling," *Journal of Dynamic Systems, Measurement, and Control* .

[23] Wadhwa, N., Rubinstein, M., Durand, F., and Freeman, W. T., "Phase-based video motion processing," *ACM Trans. Graph. (Proceedings SIGGRAPH 2013)* **32**(4) (2013).

[24] Chen, J. G., Wadhwa, N., Cha, Y.-J., Durand, F., Freeman, W. T., and Buyukozturk, O., "Modal identification of simple structures with high-speed video using motion magnification," *Journal of Sound and Vibration* **345**, 58–71 (2015).

[25] Ghazi, R. M., Chen, J., and Buyukozturk, O., "Ising graphical models for structural health monitoring with dense sensor networks," *Journal of Mechanical Systems and Signal Processing* (in review).

[26] Hastie, T., Tibshirani, R., and Friedman, J., [*The Elements of Statistical Learning: Data Mining, Inference, and Prediction*], Springer Series in Statistics, second ed. (2009).